Drug Development and Industrial Pharmacy, 34:817–826, 2008

ISSN: 0363-9045 print / 1520-5762 online
DOI: 10.1080/03639040801926063

Development of a Cyclodextrin-Based Nasal Delivery System for Lorazepam

Mario Jug and M. Bećirević-Laćan
Department of Pharmaceutics, Faculty of Pharmacy and Biochemistry,
University of Zagreb, Zagreb, Croatia

A new drug delivery system containing hydroxypropyl-β-cyclodextrin (HP-β-CD) and a mucoadhesive polymer was developed with the aim to overcome the limitations connected with the nasal application of drugs with low water solubility. Lorazepam, free or as cyclodextrin inclusion complex, was loaded into mucoadhesive microparticles by spray drying, using hydroxypropylmethyl cellulose (HPMC), carbomer, and HPMC/carbomer interpolymer complex (IPC) as mucoadhesive components. Differential scanning calorimetry (DSC) indicated the presence of drug crystalline areas in microparticles loaded with free lorazepam, whereas in those loaded with HP-β-CD inclusion complex, the drug was amorphous. Zeta potential measurement revealed that the polymer was the main component on the surface of the microparticles. The swelling rate and mucoadhesive properties of the microparticles were determined by the polymer type used in formulation. IPC- and carbomer-based microparticles showed superior swelling rate and mucoadhesion compared with the HPMC-based microparticles ($p < .05$). Drug loading into the polymer matrix decreased the swelling rate as well as the mucoadhesive properties of microparticles ($p < .05$), whereas the presence of HP-β-CD in the matrix did not induce any additional reduction of those parameters ($p > .05$). The in vitro dissolution studies demonstrated that the microparticles containing the lorazepam inclusion complex displayed 1.8–2.5 times faster drug release compared with those containing free lorazepam. The change in the drug release rate could be connected with improved drug solubility inside the polymer matrix due to inclusion complex formation, as well as to the reduction in crystallinity following complexation, as confirmed by DSC studies.

Keywords lorazepam; hydroxypropyl-β-cyclodextrin; mucoadhesion; nasal delivery

INTRODUCTION

Lorazepam, a potent benzodiazepine, has been shown to have marked anxiolytic and sedative properties. This drug is often used for preanesthetic medication; it is useful for managing status epilepticus, chemotherapy-induced nausea, and vomiting. Because of its poor water solubility and extensive metabolism in liver to pharmacologically inactive glucuronides, lorazepam oral therapy is connected with a slow onset of drug action (Rey, Treluyer, & Pons, 1999). Thus, there is considerable interest in exploring other ways of lorazepam application and developing suitable dosage forms that would lead to faster onset of action.

Administration of drugs by the nasal route is a promising method for achieving rapid systemic delivery. Nasal mucosa is relatively permeable and highly vascularized, providing rapid absorption of the applied drug and thereby avoiding degradation in the gastrointestinal tract and first-pass metabolism in liver. Rapid absorption into the systemic circulation after nasal administration has been demonstrated with several drugs active in the central nervous system (Constantino, Illum, Brandt, Johnson, & Quay, 2007). Hence, because of the simple and convenient application procedure, nasal application may be an attractive option for drug delivery in an emergency situation such as status epilepticus. The possibility of direct nose-to-brain transport of small lipophilic molecules via the olfactory region of the nasal cavity may be an additional advantage of nasal drug application (Illum, 2004).

Intranasal administration of lorazepam 2-mg dose to healthy volunteers resulted in faster absorption than intramuscular administration of the same dose, with bioavailability of 77.7 ± 11.1% (Wermeling, Miller, Archer, Manaligod, & Rudy, 2001), but concentration–time profiles for intranasal delivery demonstrated evidence of a double peak in several subjects, suggesting partial oral absorption. The mucociliary clearance of the applied drug formulation from the site of deposition resulted in short residence time for absorption. Mucoadhesive drug delivery systems can be used to increase the nasal residence time, thus allowing a longer absorption time, and to achieve more intimate contact with the nasal mucosa, which results in a higher concentration gradient and subsequent increased absorption (Ugwoke, Agu, Verbeke, & Kinget, 2005). Some mucoadhesive polymers, such as carbomers and chitosan, may act as absorption enhancers because they trigger paracellular drug transport (Li et al., 2006).

Address correspondence to Mario Jug, Department of Pharmaceutics, Faculty of Pharmacy and Biochemistry, University of Zagreb, A. Kovacica 1, 10 000 Zagreb, Croatia. E-mail: mjug@pharma.hr

Water solubility is another parameter that affects nasal bioavailability of small lipophilic molecules. It is therefore necessary to increase drug solubility to allow the delivery of a therapeutically relevant dose (Constantino et al., 2007). One of the possible approaches is the formation of drug/cyclodextrin inclusion complexes. Cyclodextrins may be used to improve nasal bioavailability of lipophilic drugs, because the formation of dynamic, noncovalent inclusion complexes can enhance apparent water solubility of the drug with no influence on their permeability across biological membranes. Also, cyclodextrins may interact with the lipophilic components of biological membranes changing their permeability. Clinical trials have shown that nasal application of cyclodextrins to humans was well tolerated, with only minor adverse effects (Merkus et al., 1999). Hydroxypropyl-β-cyclodextrin (HP-β-CD) showed superior tolerability compared with other cyclodextrin derivates, because the long-term nasal application of 20% HP-β-CD dose had no influence on the integrity of the mucosa in rats (Asai et al., 2002). Also, studies involving human cell cultures have shown that HP-β-CD has no significant cilio-inhibitory effect (Agu et al., 2000).

Based on previous information, the aim of this work was to develop and evaluate a new microparticulate delivery system containing cyclodextrin and a mucoadhesive polymer intended for nasal application of lipophilic drugs, such as lorazepam. Simultaneous implementation of the cyclodextrin inclusion complex and mucoadhesive polymer into a unique delivery system may result in a combination of the benefits of each component regarding their potential to enhance nasal bioavailability of the drugs.

MATERIALS AND METHODS

Lorazepam was kindly donated by Belupo (Koprivnica, Croatia). HP-β-CD with average substitution degree per anhydroglucose unit of 0.9 was used as received (Wacker Chemie GmbH, Munich, Germany). Hydroxypropylmethyl cellulose (HPMC, Metolose® 90 SH; η=4,000 mPa s; Shin-Etsu Chemical Co., Ltd., Tokyo, Japan) and carbomer (Carbopol® 941, η = 4,000 –10,000 mPa s; Noveon, Inc., Cleveland, OH, USA) were used as mucoadhesive polymers. All other materials and solvents used were of analytical reagent grade.

Preparation of the Solid Complex

For preparation of the inclusion complex ($L_{HP\text{-}\beta\text{-}CD}$), lorazepam (0.642 g), and an equimolar amount of HP-β-CD (3.0 g) were separately dissolved in 50 mL of 96% ethanol and 50 mL of water, respectively. The solutions were mixed together and stirred (600 rpm) for next 24 h at ambient temperature to obtain complexation equilibrium. The obtained solution was subjected to spray drying using a Büchi 190 Mini Spray Dryer (Flawil, Switzerland) with a standard 0.5-mm nozzle. The drying conditions were as follows: flow rate 0.25 L/h^{-1}, inlet temperature 150°C, outlet temperature 100°C, and air flow rate 700 NL/h.

The ethanol/water solution of the drug without HP-β-CD was also prepared as per the same procedure, and the solid product (L_0) was isolated by spray drying as described above.

Preparation of the Mucoadhesive Microparticles

The microparticles were prepared by spray drying using HPMC, carbomer, and HPMC/carbomer interpolymer complex (IPC) as mucoadhesive components. IPC was previously prepared by mixing 1% (wt/vol) aqueous solutions of HPMC and carbomer in the 1:1 volume ratio. The obtained solution was stirred uniformly for 1 h and subjected to spray drying to prepare IPC in solid state. The drying conditions were as described earlier.

For the preparation of microparticles (ML1–ML6), the polymer (0.5 g) was dissolved in 50 mL of water. Lorazepam (0.5 g) or the cyclodextrin complex containing the same amount of the drug was dissolved in 50 mL of 96% ethanol and mixed with the polymer solution. The obtained solution was uniformly stirred (600 rpm) at room temperature for 1 h and subjected to spray drying under the condition described earlier. Composition of the microparticles formulations are given in Table 1. The mass ratio of lorazepam, free or in complex form, and mucoadhesive polymer was 1:1 in all prepared microparticles.

Drug-free microparticles (M_{HPMC}, $M_{carbomer}$, and M_{IPC}) were prepared according the same procedure, omitting the drug (free or as cyclodextrin inclusion complex) from the preparation.

Determination of the Drug Content in Solid Products

The drug content in prepared products was determined spectrophotometrically after extraction from the samples with 96% ethanol under sonication in an ultrasonic bath (Branson B1210E-DTH, Danbury, CT, USA). After filtration through a 0.20-μm Millipore® membrane filter, lorazepam concentration in the samples was determined spectrophotometrically (Ultrospec Plus LKB UV/VIS spectrophotometer, Pharmacia, Uppsala, Sweden) at the drug absorption maximum wavelength of 230 nm (Popović, Sladić, Stefanović, & Pfendt, 2003). Preliminary studies showed that the presence of mucoadhesive polymers and HP-β-CD in the samples did not interfere with lorazepam absorbance at this wavelength. The limit of lorazepam quantification (LOQ) was determined to be 1.0 μg/mL. The working range of the method was 2–10 μg/mL, and Beer's law was verified over this concentration range (r^2 = .9991). The repeatability of the analysis expressed as the relative standard deviation (*RSD*) was ≤.99% and the recovery value ranged from 99.3 to 100.4%. Therefore, this method was considered to be suitable for the purpose of this study.

TABLE 1
Composition, Drug Loading, Mean Spherical Diameter, and Zeta Potential Values (ζ) of Prepared Microparticles

	Polymer	Drug	Drug Loading[a]/(%)	Mean Spherical Diameter/(μm)	ζ/(mV)
M_{HPMC}		–	–	2.65 ± 1.21	–1.6 ± 2.0
ML1	HPMC	Lorazepam	100.36 ± 1.64	2.73 ± 1.33	–2.1 ± 0.7
ML2		Inclusion complex	95.39 ± 1.67	2.62 ± 1.17	–1.1 ± 1.3
$M_{carbomer}$	Carbomer	–	–	2.38 ± 1.19	–23.7 ± 1.0
ML3		Lorazepam	101.46 ± 0.29	2.54 ± 1.29	–25.1 ± 1.1
ML4		Inclusion complex	94.92 ± 1.80	2.67 ± 1.18	–27.6 ± 0.8
M_{IPC}	IPC	–	–	2.43 ± 1.31	–17.7 ± 1.6
ML5		Lorazepam	101.78 ± 1.83	2.59 ± 1.28	–19.6 ± 1.0
ML6		Inclusion complex	100.10 ± 0.78	2.97 ± 1.22	–17.7 ± 2.0

[a] The ratio between actual and theoretical drug content in the microparticles expressed as percentage.

The drug loading was calculated as the ratio between the actual and theoretical lorazepam content in the microparticles, expressed as percentage.

Particle Size Determination

A microscopical imaging analysis was applied for the determination of particle size and distribution using an Olympus BH-2 microscope, equipped with a computer-controlled image analysis system (Optomax V, Cambridge, UK).

Differential Scanning Calorimetry

Differential scanning calorimetry (DSC) thermograms of the solid products were recorded on a Perkin Elmer DSC 7 (Wellesley, MA, USA). The instrument was calibrated with indium and zinc prior to analysis of samples under dry nitrogen purge at flow rate of 35 mL/min. All accurately weighed samples (2–5 mg) were placed in sealed aluminum pans and scanned at a heating rate of 10°C/min over the temperature range of 20–220°C.

Fourier Transformed Infrared Spectroscopic Studies

The Fourier transformed infrared (FTIR) spectra of the solid products were recorded by Perkin-Elmer spectrum GX spectrometer (Wellesley, MA, USA). The samples were prepared by the potassium bromide disc method (2-mg sample in 200-mg KBr) and scanned for absorbance in range of 4,000–500 cm^{-1} at 1 cm^{-1} resolution.

Zeta Potential Measurement

Zeta potential of spray-dried components (lorazepam, HPMC, carbomer, IPC) and the prepared microparticles were determined by photon-correlation spectroscopy (Zetasizer 3,000 HSA, Malvern Instruments, Malvern, UK) in 10 mM NaCl solution (pH 6.7) at 25°C.

Swelling Studies

Swelling properties of prepared microparticles were investigated measuring water uptake gravimetrically. About 100 mg of the prepared microparticles as well as drug-free microparticles (HPMC, carbomer, IPC) were compressed into discs of 1 cm diameter by means of a hydraulic press (Glenrothes, UK), applying a compression pressure of 160 kPa/cm. The preweighed discs were immersed into water thermostated at 37°C. At predetermined times, the swollen discs were removed from the media, blotted to remove excess water, and weighted. The dynamics of water uptake was expressed as weight gain (w_p) of the swelled matrix, calculated as a ratio between the amount of the water remained in the swelled matrix for a given period of time and the initial weight of the dry matrix. The kinetics of water uptake was analysed to equation:

$$w_p = K_p \times t^{n_p}, \tag{1}$$

where w_p is the weight gain of the swelled matrix; K_p is the kinetic constant of water penetration; t is penetration time; and n_p is an exponent that depends on the water penetration mechanism.

In Vitro Mucoadhesion Test

To evaluate the microparticles mucoadhesive properties, we performed a tensile study using bovine nasal mucosa. Prepared microparticles as well as plain polymers (HPMC, carbomer, IPC) were compressed into discs as described earlier. The discs were attached to the stainless steel support connected to a precise balance (Sartorius BP 221S, Goettingen, Germany) using cyanoacrylate glue. The bovine nasal mucosa was fixed to glass dish mounted on the mobile support. The mucosa surface was wetted with 100 μL of simulated nasal fluid (8.77 g NaCl, 2.98 g KCl, and 0.59 g $CaCl_2$/1,000 mL of demineralized water; pH 6.4) and brought in contact with the sample. The sample and the tissue were left in contact for 5 min, allowing the formation of a mucoadhesive bond. The force of detachment was measured as a function of displacement, by lowering the mobile support at a constant rate of 5 mm/min until total separation of the components was achieved. The work of mucoadhesion (*W*) was calculated as the area under the force/distance curve.

In Vitro Dissolution Studies

In vitro dissolution study employed standard Franz diffusion cell (PermeGear, Hellertown, USA) with diffusion area of 10.18 cm^2 and the acceptor compartment volume of 16 mL. Lorazepam, inclusion complex, or prepared microparticles containing 5 mg of the drug were applied evenly across the prehydrated semipermeable membrane (Medicell Dialysis Tubing, MWCO 600 Da) clamped between the donor and acceptor compartments. The membrane was wetted with 50 μL of simulated nasal fluid containing 1% of the mucine. After the sample was applied, the donor compartment of the Franz diffusion cells was closed with Parafilm® "M" sealing film (American National Can Company, Chicago, IL, USA) to avoid evaporation of the release medium and to allow the establishment of constant relative humidity around the sample. Phosphate buffer (pH 7.4) in the acceptor compartment was continuously stirred at 600 rpm using a magnetic stirrer. The cells were thermostated at 37ºC. At set time intervals, aliquots of the acceptor phase were removed and assayed for the drug content spectrophotometrically (λ = 230 nm) after suitable dilution with 96% ethanol according to the method described earlier. The removed samples were immediately replaced with an equal quantity of prewarmed receptor medium. Cumulative corrections were performed for previously removed samples.

Statistical Analysis

All values are expressed as mean ± *SD* of *n* separate experiments. Data were compared for single comparison by Student's *t* test and for multiple comparisons by one-way ANOVA, followed by Bonferroni's multiple comparison test. Values of $p < .05$ were considered significant. Calculations were performed using the GraphPad Prism program (GraphPad Software, Inc., San Diego, CA; http://www.graphpad.com).

RESULTS AND DISCUSSION

Inclusion Complex Formation in the Solid State

Preliminary solubility studies indicated formation of a soluble lorazepam/HP-β-CD inclusion complex with 1:1 stoichiometry and apparent stability constant, K_s = 281.25 ± 21.51 M^{-1}. Therefore, the inclusion complex in the solid state ($L_{HP\text{-}\beta\text{-}CD}$) was prepared by spray drying of the drug and cyclodextrin solution in an equimolar ratio.

Inclusion complex formation in the solid state was evaluated using thermal (DSC) and spectral (FTIR) analyses. The obtained DSC thermograms are shown in Figure 1. The thermogram of crystalline lorazepam showed a fusion endothermic peak at 182.6°C (ΔH = 192.0 J/g). There are three known lorazepam polymorphs and the thermogram of the crystalline drug indicated the presence of the most stabile polymorph (b) (Chauvet, Kadoura, & Masse, 1992). The high value of fusion enthalpy for crystalline lorazepam could be explained by lorazepam dimer formation in the solid state. Lack of a substituent on the N1 atom of the diazepine ring offers the possibility of hydrogen bonding between nitrogen on N1 and the oxygen atom of the carbonyl group of an adjacent molecule. Also, hydrogen bonding between the hydroxyl group at position C3 of the diazepine ring and the carbonyl group of an adjacent molecule could be assumed. Dimer formation additionally stabilized the crystal lattice structure, so higher energy was required to transfer the crystal to the liquid state (Van den Mooter, Van den Brande, Agustijns, & Kinget, 1999).

In the thermogram of spray-dried lorazepam, the drug fusion peak was also evident, but the fusion peak was shifted to lower temperatures with a decreased fusion enthalpy value (176.8°C; ΔH = 121.2 J/g). During the spray-drying procedure, solvent evaporation was very fast and dimer formation during lorazepam crystallization was partially obscured. Lower energy was therefore necessary for the fusion of spray-dried lorazepam, and the fusion peak was shifted to lower temperatures with decreased fusion enthalpy. The endothermic fusion peak corresponding to drug melting was still evident in the thermogram of the lorazepam/HP-β-CD physical mixture (175.9ºC; ΔH = 36.9 J/g). The change of the lorazepam fusion peak position and intensity in the case of the drug/HP-β-CD physical mixture could be explained by thermally induced interaction during the DCS experiment (Aigner, Hassan,

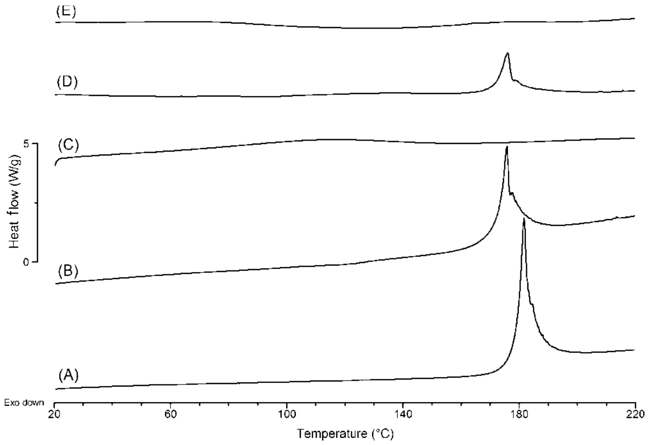

FIGURE 1. Differential scanning calorimetry (DSC) thermograms of crystalline lorazepam (A), spray-dried lorazepam (B), hydroxypropyl-β-cyclodextrin (HP-β-CD) (C), equimolar drug/ HP-β-CD physical mixture (D), and spray-dried inclusion complex (E).

Berkesi, Kata, & Eros, 2005). In the thermogram of the spray-dried complex, lorazepam fusion peak was completely absent. This phenomenon is generally considered to be indicative of drug amorphization and/or inclusion complex formation (Mura, Zerrouk, Faucci, Maestrelli, & Chemtob, 2002). Inclusion complex formation hampered lorazepam crystallization during the spray-drying procedure, probably for sterical reasons leading to the drug amorphous state.

The FTIR spectra of crystalline lorazepam (Figure 2) could also be attributed to the polymorph (b) (Chauvet et al. 1992). The position and intensity of all absorption bands in the spectra of the spray-dried drug were the same as for crystalline lorazepam, except for the doublet at 1,159.6 and 1,132.3 cm^{-1}, corresponding to the C–OH stretching vibrations. In the case of spray-dried lorazepam, the intensity of the band at 1,159.6 cm^{-1} decreased, indicating some reorganization of the hydrogen bonds in the crystal lattice. Perhaps, very fast solvent evaporation during the spray-drying procedure partially hampered lorazepam dimer formation, causing the change in FTIR spectra. This was also confirmed by the observation based on the DSC results. In the spectra of the spray-dried inclusion complex, characteristic lorazepam absorption bands disappeared and the position of the amide carbonyl-stretching band shifted from 1,694.8 cm^{-1} (crystalline drug) to 1,705.6 cm^{-1} (spray-dried complex), whereas the intensity of the band was significantly reduced. The shift suggested breakage of intermolecular hydrogen bonds between amide carbonyl groups of two adjacent lorazepam molecules. This may be indicative of the drug monomeric dispersion formation as a consequence of lorazepam complexation with HP-β-CD. Inclusion complex formation sterically hindered lorazepam crystallization and dimer formation, thereby stabilizing the drug amorphous form (Brown, Glass, & Worthington, 2002). The inclusion complex formation also restricted vibrational motions of a drug moiety included in the cyclodextrin cavity, resulting in decreased absorption band intensity. Thus, the change in FTIR spectra of the spray-dried complex indirectly confirmed the inclusion complex formation.

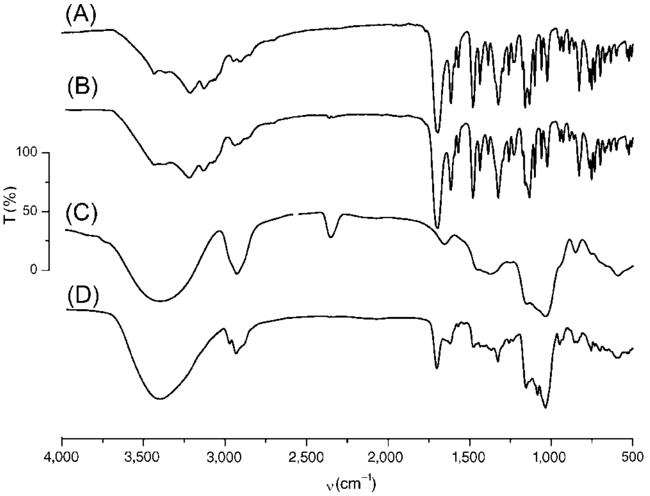

FIGURE 2. Fourier transformed infrared (FTIR) spectra of crystalline lorazepam (A), spray-dried lorazepam (B), hydroxypropyl-β-cyclodextrin (HP-β-CD) (C), and spray-dried inclusion complex (D).

Characterization of Microparticles

Lorazepam, free or as HP-β-CD inclusion complex, was loaded into mucoadhesive microparticles by spray drying. Prepared microparticles were characterized by drug content and particle size determination, DSC analysis, and zeta potential measurements. Swelling and mucoadhesive properties of prepared microparticles were also evaluated.

Drug content determination revealed high lorazepam loading in the microparticles with average spherical diameters towards 3.0 μm (Table 1). The particle size distribution of all prepared microparticles followed a log-normal distribution, with less than 10% of microparticles larger than 5 μm. The presence of larger particles could be attributed to aggregation of microparticles during the spray-drying procedure. HP-β-CD did not significantly affect the drug loading value and mean spherical diameter of the microparticles ($p > .05$).

To evaluate internal structure modification, we analyzed prepared microparticles by DSC and the obtained thermograms were compared with those of spray-dried lorazepam (Figure 3). In thermograms of microparticles (ML1–ML6), broad endothermic peaks could be observed in the range of 35–110°C corresponding to the evaporation of absorbed water. In the thermograms of microparticles loaded with lorazepam (ML1, ML3, and ML5), endothermic drug fusion peaks were still evident but were shifted to lower temperatures with decreased fusion enthalpy (Figure 3). This could be attributed to lorazepam incorporation into the polymeric matrix of the microparticles and also to the thermally induced drug-polymer interaction during DSC experiment (Dash, Khin-Khin, & Suryanarayanan, 2002).

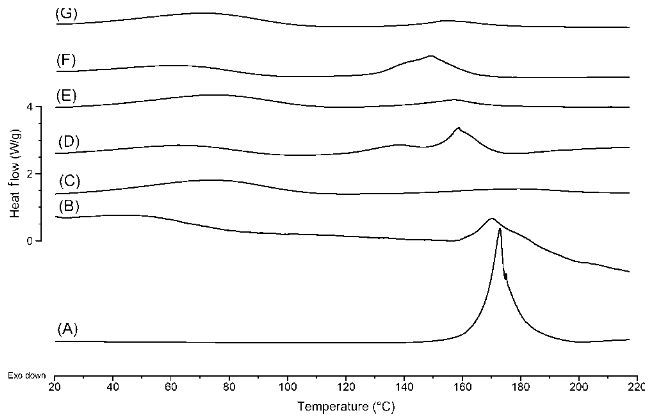

FIGURE 3. Differential scanning calorimetry (DSC) thermograms of spray-dried lorazepam (A) and microparticles ML1 (B), ML 2 (C), ML3 (D), ML4 (E), ML5 (F), and ML6 (G).

According to these results, the presence of lorazepam microcrystalline areas in microparticles ML1, ML3, and ML5 could still be assumed. In the thermograms of microparticles loaded with the lorazepam/HP-β-CD inclusion complex (ML2, ML4, and ML6), the endothermic drug fusion peak was absent. It may be concluded that loading of the inclusion complex into microparticles has no affect on the inclusion complex structure because lorazepam, as a lipophilic drug, would show higher affinity for the lipophilic central cavity of the cyclodextrin molecule than for the interaction with the hydrophilic polymer of the microparticle matrix.

To investigate surface characteristics of the prepared microparticles, we performed zeta potential measurements. Changes of the zeta potential may also point to interactions between the components of microparticles (Harnsilawat, Pongsawatmanit, & McClements, 2006).

Zeta potential values of prepared microparticles are presented in Table 1. In the case of blank HPMC microparticles (M_{HPMC}), the zeta potential value was close to zero due to the nonionic nature of the polymer. The presence of charged carboxyl groups on the particle surface gave rise to negative zeta potential values of blank carbomer microparticles ($M_{carbomer}$). Zeta potential of blank IPC microparticles (M_{IPC}) was lower compared with that of blank carbomer microparticles, confirming the IPC formation. Simultaneous establishment of intermacromolecular hydrogen bonds between carboxyl groups of the carbomer and hydrogen groups of HPMC reduced the number of charged carboxyl groups at the particle surface, thereby reducing the zeta potential value of drug-free IPC microparticles.

Comparing the zeta potential values for blank and drug-loaded microparticles, it is possible to determine the main component on the microparticle surface. Zeta potential values of blank and drug-loaded HPMC microparticles (M_{HPMC} and ML1, respectively) do not differ significantly ($p > .05$). The same conclusion can be made comparing the zeta potential value of blank and drug-loaded carbomers and IPC microparticles ($M_{carbomer}$ vs. ML3 and M_{IPC} vs. ML5, respectively). This indicated that the polymer was the dominant component on the surface of microparticles and that drug microcrystalline areas, proven by DSC, are located inside of the polymer matrix. The presence of HP-β-CD in the microparticles (ML2, ML4, and ML6) has no significant influence on the zeta potential value. This may be attributed to the nonionic nature of cyclodextrin. Also, HP-β-CD possesses numerous hydroxyl groups that may interact with proton acceptor groups of the polymer (carboxylic groups of carbomer and ether groups of HPMC). This interaction may result in coating of the polymer chain around the cyclodextrin molecule. Hence, the polymer remained the main component on the particle surface, contributing to the zeta potential value.

The rate and extent of water uptake by the polymer matrix are crucial parameters, significantly affecting the mobility of polymer chains. Thus, water-uptake characteristics would have a significant impact on mucoadhesive bond formation and drug release from the matrix. The water-uptake profiles of blank (M_{HPMC}, $M_{carbomer}$, and M_{IPC}) and drug-loaded microparticles (ML1–ML6) are presented in Figure 4.

To better understand the dominant mass transport processes upon exposure of polymeric matrixes to water, the mathematical model described by Equation 1 was applied to the experimental data. The determined kinetic constant (K_p) and water-uptake exponent (n_p) values are given in Table 2. According to the n_p value, it is possible to determine the main water transport mechanism. The value of n_p near 0.5 for the blank HPMC matrix (M_{HPMC}) indicated that water diffusion is

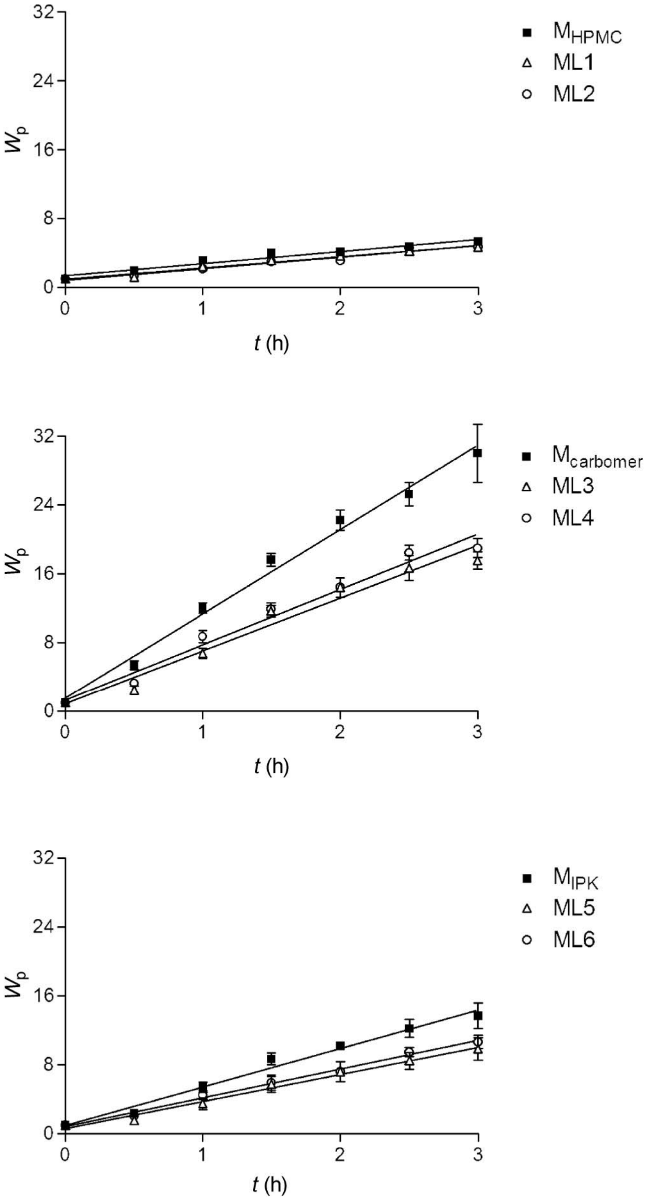

FIGURE 4. Weight gain (w_p) of the samples as a function of the swelling time (mean ± *SD*; $n = 5$).

TABLE 2
The Kinetic Constants of the Water Uptake (K_p), Water Penetration Exponents (n_p), in vitro Mucoadhesion Expressed as Work of Adhesion (W), and Drug Release Constants (k) for the Prepared Microparticles

Sample	$K_p(h^{-n})$	n_p	W(μJ)	$k \times 10^3$(mg min^{-1})
L_0	–	–	–	2.36 ± 0.05
$L_{HP\text{-}\beta\text{-}CD}$	–	–	–	15.05 ± 0.24[e]
M_{HPMC}	0.20 ± 0.02	0.54 ± 0.04	71.78 ± 13.97	–
ML1	0.14 ± 0.04	0.75 ± 0.06	45.41 ± 3.72[a]	7.24 ± 0.12
ML2	0.08 ± 0.04	0.71 ± 0.06	31.85 ± 8.44[a]	14.18 ± 0.18[f]
$M_{carbomer}$	0.32 ± 0.03	0.95 ± 0.05	137.98 ± 26.25	–
ML3	0.22 ± 0.08	1.04 ± 0.11	85.52±13.66[b]	8.09 ± 0.15
ML4	0.21 ± 0.06	0.98 ± 0.09	80.80±13.42[c]	14.56 ± 0.28[f]
M_{IPC}	0.18 ± 0.04	0.97 ± 0.07	129.12 ± 8.60	–
ML5	0.15 ± 0.04	1.06 ± 0.06	76.12 ± 7.13[d]	4.15 ± 0.09
ML6	0.14 ± 0.03	0.91 ± 0.04	72.97±21.62[d]	10.62 ± 0.23[f]

[a] Statistically significant difference compared to M_{HPMC} ($p < .05$).
[b] Statistically significant difference compared to $M_{carbomer}$ ($p < .05$.).
[c] Statistically significant difference compared to $M_{carbomer}$ ($p < .01$).
[d] Statistically significant difference compared to M_{IPC} ($p < .01$).
[e] Statistically significant difference compared to L_0 ($p < .05$).
[f] Statistically significant difference compared with HP-β-CD free microparticles based on the same polymer ($p < .05$).

the predominant mass transport phenomenon (Brazel & Peppas, 1999). After contact of the matrix with the swelling medium, water molecules diffuse between HPMC chains causing formation of a gel layer around the dry core.

In the case of the carbomer blank matrix ($M_{carbomer}$), the n_p value around 1.0 indicated that water uptake could be classified as case II transport. This suggested that relaxation of polymer chains facilitated water uptake. In contact with water, carboxylic groups of the polymer will dissociate and set up an electrostatic repulsion, which tends to expand the chain network. Also, because of the ionized carboxyl group inside the polymer matrix, an osmotic pressure difference existed between internal and external solutions of the gel network (Dittgen, Durrani, & Lehmann, 1997). Osmotic pressure additionally contributed to the water-uptake rate. Therefore, the K_p value for $M_{carbomer}$ was higher compared with that of M_{HPMC}. The n_p value for the blank IPC matrix (M_{IPC}) was similar to that for the blank carbomer matrix. This indicated that water uptake into the IPC blank matrix followed the same mechanism, but the water uptake rate was lower. The IPC formation occupied carboxylic groups and thereby restricted electrostatic repulsion forces and the osmotic pressure difference, leading to slower water uptake.

Incorporation of the drug into the polymeric matrix (ML1, ML3, and ML5) decreased the water-uptake rate in all cases (Table 2), probably because the hydrophobic lorazepam nature restricted water transport inside the matrix. The uniformly distributed drug microcrystalline areas will occupy the free volume of the swollen hydrogel and create a tortuous path for the water to penetrate. In the case of ML1, the drug presence changed the water-uptake mechanism. According to the n_p value, it may be classified as anomalous transport, suggesting simultaneous contribution of water diffusion and polymer chain relaxation to the water penetration rate. In the case of ML3 and ML5 samples, the n_p value indicated that the drug presence in the matrix did not change the water penetration mechanism.

The presence of HP-β-CD in the samples (ML2, ML4, and ML6) slightly reduced the water-uptake rate compared with cyclodextrin-free microparticles (ML1, ML3, and ML5). Pronounced erosion of those matrices was also observed. Cyclodextrins may interact with polymer chains through noninclusion complexes' formation (Rodríguez-Tenreiro, et al., 2004), causing a change in the water-uptake rate. Also, the cyclodextrin–polymer interaction may decrease the apparent viscosity of the formed gel layer (Boulmedarat, Grossiord, Fattal, & Bochot, 2003; Pose-Vilarnovo et al. 2004), thus facilitating matrix erosion.

The n_p values for microparticles, where the drug was loaded as the cyclodextrin complex (ML2, ML4, and ML6), are similar to cyclodextrin-free microparticles based on the same polymer (ML1, ML3, and ML5). This indicated that HP-β-CD caused no significant change in the water-uptake mechanism.

The influence of drug loading and HP-β-CD presence on mucoadhesive properties of the microparticles was evaluated by comparing the work of adhesion value for blank and drug-loaded microparticles. The results of in vitro mucoadhesion determination are presented in Table 2. The polymer used for the preparation of microparticles determined their mucoadhesive properties. Mucoadhesive properties of the blank HPMC microparticles (M_{HPMC}) were less pronounced compared that of blank carbomer and IPC microparticles ($p < .05$). HPMC is a neutral polymer with linear structure. In contact with the mucosa, swelling of the polymer matrix occurred, followed by interpenetration of mucine and HPMC strands. A weak mechanical bond was thereby formed. Modest swelling properties of the HPMC matrix, demonstrated by water-uptake studies, restricted the formation of mucoadhesive bonds, leading to low work of adhesion values.

Carbomer is a cross-linked polymer and the large number of carboxyl groups contributed to the high water-uptake rate, leading to fast swelling of the polymer matrix. Pronounced swelling and cross-linked structure of the carbomer contributed to the formation of a stabile mechanic mucoadhesive bond that could be further stabilized by hydrogen bonds (Edsman & Hägerström, 2005). IPC was formed by cooperative hydrogen bonds' formation between carbomer and HPMC strands. This resulted in the formation of a stabile, ladder-type structure (Nurkeeva, Mun, & Khutoryanskiy, 2003). Interpenetration of mucine strands into this formed structure could lead to the formation of a strong mucoadhesive bond. Therefore, the mucoadhesive properties of IPC and carbomer drug-free microparticles did not differ significantly ($p > .05$).

Lorazepam incorporation in the polymer matrix reduced the mucoadhesive properties of microparticles (Table 2). This could be contributed to the lower water-uptake rate observed during the swelling studies. Slower hydratation restricted the mobility of polymer chains and thereby obscured the formation of mucoadhesive bonds. Also, the presence of the drug molecule could prevent the formation of electrostatic or hydrogen bonds, which are responsible for stabilization of the mucoadhesive bond (Ikinçi et al., 2000). The presence of cyclodextrin in the polymer matrix caused no additional reduction of microparticles mucoadhesion ($p > .05$). This could be explained by the results of zeta potential measurements, which indicated that the polymer was the main component on the surface of the microparticles providing mucoadhesive properties.

In Vitro Drug Release Studies

Drug release experiments were performed using the standard Franz diffusion cell. This model allows slow hydratation of the sample in a humid environment, conditions designed to be similar to those encountered in the nasal cavity (El-Hameed & Kellaway, 1997). The release of the drug from prepared solid products included several steps, such as dissolution/release of the drug into the hydrodynamic layer on the membrane surface, followed by drug diffusion across the semipermeable membrane to the acceptor compartment of the Franz diffusion cell. Both processes made a contribution to the overall dissolution rate. The semipermeable membrane had the molecular weight cut-off value of 600 Da, so lorazepam would have been able to pass through freely. Lorazepam release profiles from the prepared solid products are presented in Figure 5. Drug release followed the zero-order kinetic model ($r^2 > .99$ for all samples). The corresponding drug release rate constants are presented in Table 2.

The main parameter affecting the lorazepam in vitro release rate was the drug solubility. During the experiment, no sink conditions in the donor compartment of the Franz diffusion cell were provided. Because of low lorazepam solubility, only limited amounts of the drug were available for diffusion in the receptor phase. Lipophilic properties of the lorazepam molecule remarkably hindered the drug transport across the hydrodynamic layer on the membrane surface. This led to a low release rate constant for spray-dried lorazepam (L_0).

Lorazepam incorporation into microparticles (ML1, ML3, and ML5) enhanced the drug release rate (Table 2). Upon contact of the microparticles with dissolution media, swelling of the polymer occurred, resulting in the formation of a gel layer around the dry core of the microparticles. Additional uptake of dissolution media into microparticles leads to erosion of the swollen gel layer. Dissolution medium uptake into microparticles was also followed by the drug dissolution. The presence of the hydrophilic polymer facilitated, to some extent,

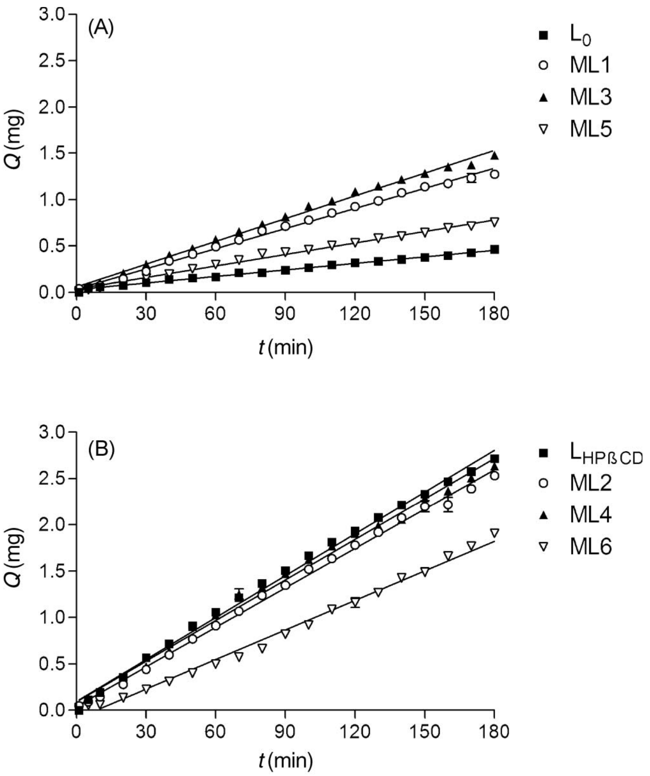

FIGURE 5. Dissolution profiles of the drug from prepared solid products without (A) and with (B) hydroxypropyl-β-cyclodextrin (HP-β-CD) (mean ± *SD*; *n*=5).

the wetting of drug particles, providing a lower energy pathway for drug dissolution. Diffusion of the drug across the swollen polymer layer and erosion of the microparticles controlled the drug release rate.

Although the swelling characteristics of HPMC and carbomer matrices differ significantly (Table 2), the enhancing effect of carbomer on the lorazepam release rate was similar to that of HPMC, probably because the drug solubility was the rate-limiting step that controlled drug release. Therefore, lorazepam release rate constants from ML1 and ML3 microparticles were similar. In the case of IPC microparticles (ML5), the drug release rate was lower compared with that of HPMC and carbomer microparticles. This may be explained in terms of the polymer network mesh size and increased tortuousness of the drug diffusional path due to IPC formation. Therefore, the IPC-based matrix provided a more controlled release of the drug with a lower drug dissolution rate value.

The drug release constant for the lorazepam inclusion complex ($L_{HP\text{-}\beta\text{-}CD}$) was 6.4-fold higher compared with spray-dried lorazepam (L_0), indicating that the inclusion complex formation significantly increased the in vitro drug dissolution rate (Table 2). This may be explained in terms of improved drug solubility due to inclusion complex formation. Also, HP-β-CD facilitated the transport of the drug through the hydrodynamic layer on the membrane surface, acting as a carrier by keeping the lipophilic drug molecules in solution and delivering them to the membrane surface. Because of high molecular weight, permeation of the inclusion complex across the semipermeable membrane could not be assumed. The drug in the complex was in rapid dynamic equilibrium with the “free” drug, thus continuously supplying lorazepam molecules to the membrane in a diffusible form. This increased the drug concentration gradient over the membrane, which led to higher drug concentrations in the acceptor compartment.

Cyclodextrin complexation also significantly increased the lorazepam release rate from the microparticles (Table 2). This could be attributed to enhanced lorazepam solubility in the swollen polymer matrix upon inclusion complex formation. Also, the amorphous state of the drug in the microparticles containing HP-β-CD, proven by DSC analysis, additionally contributed to faster drug release. The rate constants of lorazepam release from the HPMC and carbomer-based microparticles (ML2 and ML4, respectively) were only slightly lower compared with that of the inclusion complex (L_0). The swollen gel layer on the microparticles surface produced an additional diffusional pathway, thereby reducing the overall lorazepam release rate. But, complexation of the drug with hydrophilic cyclodextrin prevented hydrophobic interactions between the drug molecules and less polar segments of the polymer chains. This increased the diffusion coefficient of the drug in the swollen gel layer (Pose-Vilarnovo et al., 2004). Faster diffusion of the drug across the swollen gel layer due to inclusion complex formation contributed to the overall drug release rate. The presence of cyclodextrin in microparticles also enhanced polymer matrix erosion, which was observed during the swelling studies. This minimized the retardant effect of the gel layer on the drug release rate. More pronounced decrease of the drug release rate compared with the inclusion complex was observed for IPC-based microparticles (ML6), probably for the reasons discussed above.

CONCLUSION

It has been demonstrated that incorporation of the cyclodextrin inclusion complex into microparticles intended for nasal delivery of lipophilic drugs can be a suitable strategy for optimizing the drug release while maintaining the mucoadhesive properties. The method of microparticles preparation was simple and easy to scale up. Inclusion complex formation in the solid state was demonstrated by DSC and FTIR studies. HP-β-CD significantly improved the lorazepam release rate from the microparticles with minimal influence on their mucoadhesion. The enhanced drug release rate may be connected with improved lorazepam solubility inside the swollen polymer matrix. Also, the drug amorphous state due to inclusion complex formation additionally contributed to faster drug release. Mucoadhesive microparticles with cyclodextrins have a great potential as a nasal delivery system, with the possibility of tailoring the release features of the drug while maintaining good mucoadhesive properties.

REFERENCES

Agu, R. U., Jorissen, M., Willems, T., den Mooter, G. V., Kinget, R., Verbeke, N., & Augustijns, P. (2000). Safety assessment of selected cyclodextrins—effect on ciliary activity using a human cell suspension culture model exhibiting in vitro ciliogenesis. *Int. J. Pharm., 193*, 219–226.

Aigner, Z., Hassan, H. B., Berkesi, O., Kata, M., & Eros, I. (2005). Thermoanalytical, FTIR and X-ray studies of gemfibrozil-cyclodextrin complexes. *J. Therm. Anal. Calorim., 81*, 267–272.

Asai, K., Morishita, M., Katsuta, H., Hosoda, S., Shinomiya, K., Noro, M., Nagai, T., & Takayama, K. (2002). The effect of water-soluble cyclodextrins on the histological integrity of the rats nasal mucosa. *Int. J. Pharm., 246*, 25–35.

Boulmedarat, L., Grossiord, J., Fattal, E., & Bochot, A. (2003). Influence of methyl-β-cyclodextrin and liposomes on rheological properties of Carbopol® 974P NF gels. *Int. J. Pharm., 254*, 59–64.

Brazel, C. S., & Peppas, N. A. (1999). Mechanism of solute transport in relaxing, swellable, hydrophylic glassy polymers. *Polymer, 40*, 3383–3398.

Brown, M. E., Glass, B. D., & Worthington, M. S. (2002). Binary systems of nifedipine and various cyclodextrins in the solid state: Thermal, FTIR XRD studies. *J. Therm. Anal. Calorim., 68*, 631–646.

Chauvet, A., Kadoura, J., & Masse, J. (1992). Etude du changement de phase solide-liquide en relation avec la stabilite thermique des formes polymorphes et pesudopolymorphes du lorazepam et identification spectrale. *J. Therm. Anal., 38*, 1593–1606.

Constantino, H. R., Illum, L., Brandt, G., Johnson, P. H., & Quay, S. C. (2007). Intranasal delivery: Physiochemical and therapeutic aspects. *Int. J. Pharm., 337*, 1–24.

Dash, A. K., Khin-Khin, A., & Suryanarayanan R. (2002). X-Ray powder diffractometric method for quantitation crystalline drug in microparticulate systems. I. Microspheres. *J. Pharm. Sci., 91*, 983–990.

Dittgen, M., Durrani, M., & Lehmann, K. (1997). Acrylic polymers. A review of pharmaceutical application. *S.T.P. Pharma. Sci., 7*, 403–437.

Edsman, K., & Hägerström, H. (2005). Pharmaceutical application of mucoadhesion for the non-oral routes. *J. Pharm. Pharmacol., 57*, 3–22.

El-Hameed, M. D., & Kellaway, I. W. (1997). Preparation and in vitro characterisation of mucoadhesive polymeric microspheres as intranasal delivery systems. *Eur. J. Pharm. Biopharm., 44*, 53–60.

Harnsilawat, T., Pongsawatmanit, R., & McClements, D. J. (2006). Characterisation of β-lactoglobulin sodium algnate interactions in aqueous solution: A calorimetry, light scattering, electrophoretic mobility and solubitity studies. *Food Hydrocoll., 20*, 577–585.

Ikinçi, G., Çapan, Y., Şenel, S., Alaaddinoğlu, E., Dalkara, T., & Hincal, A. (2000). In vitro/in vivo studies on a buccal bioadhesive tablet formulation of carbamazepine. *Pharmazie*, 55, 762–765.

Illum, L. (2004). Is nose-to-brain transport of drugs in man a reality? *J. Pharm. Pharmacol., 56*, 3–17.

Li, L., Mathias, N. R., Heran, C. L., Moench, P., Wall, D. A., & Smith, R. L. (2006). Carbopol-mediated paracellular transport enhancement in Calu-3 cell layers. *J. Pharm. Sci., 95*, 326–335.

Merkus, F. W. H. M., Verhoef, J. C., Marttin, E., Romejin, S. G., van der Kuy, P. H. M., Hermens, W. A. J. J., & Schipper, N. G. M. (1999). Cyclodextrins in nasal drug delivery. *Adv. Drug Deliv. Rev., 36*, 41–57.

Mura, P., Zerrouk, N., Faucci, M. T., Maestrelli, F., & Chemtob, C. (2002). Comparative study of ibuproxam complexation with amorphous β-cyclodextrin derivates in solution and in solid state. *Eur. J. Pharm. Biopharm., 54*, 181–191.

Nurkeeva, Z. S., Mun, G. A., & Khutoryanskiy, V. V. (2003). Interpolymer complexes of water-soluble nonionic polysaccharides with polycarboxylic acids and their applications. *Macromol. Biosci., 3*, 283–295.

Popović, G. V., Sladić, D. M., Stefanović, V. M., & Pfendt, L. B. (2003). Study on protolytic equilibria of lorazepam and oxazepam by UV and NMR spectroscopy. *J. Pharm. Biomed. Anal., 31*, 693–699.

Pose-Vilarnovo, B., Rodriguez-Tenreiro, C., dos Santos, J. F. R., Vazquez-Doval, J., Concheiro, A., Alvarez-Lorenzo, C., & Torres-Labandeira, J. J. (2004). Modulating the drug release with cyclodextrins in hydroxypropyl methylcellulose gels and tablets. *J. Control Release, 94*, 351–363.

Rey, E., Treluyer, J. M., & Pons, G. (1999). Pharmacokinetic optimisation of benzodiazepine therapy for acute seizures - Focus on delivery routes. *Clin. Pharmacokinet., 36*, 409–424.

Rodríguez-Tenreiro, C., Alvarez-Lorenzo, C., Concheiro, A., & Torres-Labandeira, J. J. (2004). Characterization of cyclodextrin-carbopol interactions by DSC and FTIR. *J. Therm. Anal. Calorim., 77*, 403–411.

Ugwoke, M. I., Agu, R. U., Verbeke, N., & Kinget, R. (2005). Nasal mucoadhesive drug delivery: Background, applications, trends and future perspectives. *Adv. Drug Deliv. Rev., 57*, 1640–1665.

Van den Mooter, G., Van den Brande, J., Agustijns, P., & Kinget, R. (1999). Glass forming properties of benzodiazepines and co-evaporate systems with poly(hydroxyethyl methacrylate). *J. Therm. Anal. Calorim., 57*, 493–507.

Wermeling, D. P. H., Miller, J. L., Archer, S. M., Manaligod, J. M., & Rudy, A. C. (2001). Bioavailability and pharmacokinetics of lorazepam after intranasal, intravenous and intramuscular administration. *J. Clin. Pharmacol., 41*, 1225–1231.